Guided Ion Beam Studies of the Reactions of Co^+ and Ni^+ with CH_3X (X = Cl, Br, I). Implications for the Metal-Methyl Ion Bond Energies

Ellen R. Fisher, L. S. Sunderlin, and P. B. Armentrout*,†

Department of Chemistry, University of Utah, Salt Lake City, Utah 84112 *(Received: February 21, 1989; In Final Form: May 31, 1989)*

Guided ion beam techniques are used to study the reactions of Co^+ and Ni^+ with the methyl halides. The only products observed in these reactions are MCH_3^+ and MX^+. Bond energies for the MCH_3^+ species are determined from all six reactions and are in good agreement with those derived from an alkane study in our laboratory. In addition, bond energies are determined for the MCl^+ species. The 298 K bond energies derived here are $D°(Co^+-CH_3) = 2.12 \pm 0.13$ eV, $D°(Ni^+-CH_3) = 1.96 \pm 0.13$ eV, $D°(Co^+-Cl) = 3.04 \pm 0.12$ eV, and $D°(Ni^+-Cl) = 2.05 \pm 0.10$ eV. Combined with literature values for the neutral metal chloride bond energies, we derive the ionization potentials for the metal chloride species, IP(CoCl) = 8.5 ± 0.2 eV and IP(NiCl) = 9.4 ± 0.1 eV. The values for the M^+-CH_3 bond energies derived here and those in the literature are compared and evaluated. In the case of Co^+-CH_3, our results conflict with those of Allison and Ridge, who also studied the reactions of Co^+ with methyl halides. We are able to resolve this discrepancy by presenting evidence that both the $Co^+(^3F)$ ground state and the $Co^+(^5F)$ first excited state react efficiently with the methyl halides.

Introduction

In 1975, Allison and Ridge (AR) made some of the first studies of gas-phase transition-metal-ion chemistry by examining the reactions of Fe^+, Co^+, and Ni^+ with CH_3Br, CH_3I, and other alkyl halides using ion cyclotron resonance (ICR) techniques.[1-3] A particularly important aspect of these studies was the thermochemical information that was derived, especially for the MCH_3^+ ion. In AR's experiments, an upper limit of $D°(Ni^+-CH_3) < 2.43$ eV $= D°(CH_3-I)$ was derived as they did not observe formation of $NiCH_3^+$ by reaction of Ni^+ with CH_3Br or CH_3I. Similarly, they did not observe $CoCH_3^+$ from the reaction of $Co^+ + CH_3Br$, but they did observe an exothermic reaction of Co^+ with CH_3I to form $CoCH_3^+$. From these data, they placed limits on the bond energy of Co^+-CH_3, $D°(CH_3-I) = 2.43$ eV $< D°(Co^+-CH_3) < 2.95$ eV $= D^0(CH_3-Br)$.[4]

Using ion beam techniques to study the reaction of Co^+ and ethane, Armentrout and Beauchamp[5] (AB) found $D°(Co^+-CH_3) = 2.65 \pm 0.17$ eV, in good agreement with AR's results. Recently, we reexamined the reaction of Co^+ with ethane[6] and found a bond energy for Co^+-CH_3 of 2.13 ± 0.15 eV, well below the lower limit set by AR. On the basis of this value, the reaction of Co^+ with CH_3I to form $CoCH_3^+$ should be *endothermic* by about 0.3 eV. There are several possible explanations for these disparities, and the present study is designed to remove the ambiguity surrounding the Co^+-CH_3 bond energy by investigating the same reactions probed by AR. Thus, this study is a continuation of our efforts to elucidate thermodynamic and mechanistic information about transition-metal hydrides and alkyls.[7,8,9] In a companion paper, we further extend this work to the state-specific reactions of atomic iron ions with the methyl halides.[10]

There have been various reports on the gas-phase chemistry of alkyl halides with both alkali-metal ions[3,11,12] and transition-metal ions.[1-3,13] Alkali-metal ions induce the dehydrohalogenation of alkyl halides via a mechanism that involves transfer of the halogen to the metal cation and generation of a positive charge at the carbon center.[3] Transition metals also dehydrohalogenate alkyl halides but are thought to do so via a metal insertion mechanism, followed by a β-hydrogen atom shift from the alkyl group to the metal.[3] Evidence indicates that the transition-metal ions Fe^+, Co^+, and Ni^+ react initially with alkyl halides with little or no barrier to form the RMX^+ intermediate. These ideas are consistent with the present results, but we also observe some rather interesting behavior in the metal halide ion products. Explanations for this reactivity involve different mechanistic and dynamic behavior than previously proposed.

Experimental Section

General. The ion beam apparatus used in these experiments has been described in detail elsewhere.[14] Cobalt and nickel ions are produced as described below. The ions are extracted from the source, accelerated, and focused into a magnetic sector momentum analyzer for mass analysis. For these experiments, ^{59}Co (100% natural abundance) and ^{58}Ni (67.8% natural abundance) were used. The mass-selected ions are decelerated to a desired kinetic energy and focused into an octopole ion guide, which traps ions in the radial direction using radio frequency electric fields. The octopole passes through a cell filled with the neutral reactant. Pressures of the neutral reactants are maintained at sufficiently low levels (0.02-0.11 mTorr) that multiple ion-molecule reactions are improbable. The octopole ion guide ensures efficient collection of ionic products and transmitted reactant ions. After exiting the reaction cell, the ions are extracted from the octopole, focused into a quadrupole mass filter for mass analysis, and detected by use of a scintillation ion detector and standard ion counting techniques. Raw ion intensities are then converted into absolute reaction cross sections as described in detail previously.[14] The uncertainties in these cross sections are estimated at ±20%.

Laboratory ion energies (lab) are converted to energies in the center-of-mass frame (CM) by using the conversion $E(\mathrm{CM}) = E(\mathrm{lab})M/(m + M)$, where m is the ion mass and M is the target molecule mass. The absolute energy scale and the corresponding full width at half-maximum (fwhm) of the ion kinetic energy

---

† NSF Presidential Young Investigator, 1984-1989. Alfred P. Sloan Fellow. Camille and Henry Dreyfus Teacher-Scholar, 1987-1992.

[1] Allison, J.; Ridge, D. P. *J. Am. Chem. Soc.* **1976**, *98*, 7445-7447.

[2] Allison, J.; Ridge, D. P. *J. Organometallic Chem.* **1975**, *99*, C11-C14.

[3] Allison, J.; Ridge, D. P. *J. Am. Chem. Soc.* **1979**, *101*, 4998-5009.

[4] Values used by AR for $D°(CH_3-I)$ and $D°(CH_3-Br)$ are slightly different from the values used here, $D°(CH_3-I) = 2.46$ eV and $D°(CH_3-Br) = 3.04$ eV, due to different literature heats of formation.

[5] Armentrout, P. B.; Beauchamp, J. L. *J. Am. Chem. Soc.* **1981**, *103*, 784-791.

[6] Georgiadis, R.; Fisher, E. R.; Armentrout, P. B. *J. Am. Chem. Soc.* **1989**, *111*, 4251-4262.

[7] Elkind, J. L.; Armentrout, P. B. *J. Phys. Chem.* **1986**, *90*, 5736-5745.

[8] Elkind, J. L.; Armentrout, P. B. *J. Phys. Chem.* **1986**, *90*, 6576-6586.

[9] Elkind, J. L.; Armentrout, P. B. *J. Phys. Chem.* **1987**, *91*, 2037-2045. Schultz, R. H.; Elkind, J. L.; Armentrout, P. B. *J. Am. Chem. Soc.* **1988**, *110*, 411-423.

[10] Fisher, E. R.; Schultz, R. H.; Armentrout, P. B. *J. Phys. Chem.*, following paper in this issue.

[11] Weiting, R. D.; Staley, R. H.; Beauchamp, J. L. *J. Am. Chem. Soc.* **1975**, *97*, 924-926.

[12] Creasy, W. R.; Farrar, J. M. *J. Chem. Phys.* **1987**, *87*, 5280-5293.

[13] Chowdhury, A. K.; Wilkins, C. L. *J. Am. Chem. Soc.* **1987**, *109*, 5336-5343.

[14] Ervin, K. M.; Armentrout, P. B. *J. Chem. Phys.* **1985**, *83*, 166-189.

0022-3654/89/2093-7375$01.50/0

TABLE I: Low-Lying States of Co^+ and Ni^+

ion	state	confign	J^a	E,^{b} eV	population^c
Co^+	a^3F	$3d^8$	4	0.000	0.520 ± 0.016
			3	0.117	0.220 ± 0.001
			2	0.198	0.104 ± 0.002
			av	0.055	0.844 ± 0.013
	a^5F	$4s3d^7$	5	0.415	0.076 ± 0.002
			4	0.499	0.040 ± 0.001
			3	0.565	0.022 ± 0.001
			2	0.613	0.013 ± 0.001
			1	0.645	0.006 ± 0.0002
			av	0.483	0.157 ± 0.013
	b^3F	$4s3d^7$	av	1.298	0.002 ± 0.0001
Ni^+	a^2D	$3d^9$	2.5	0.000	0.784 ± 0.020
			1.5	0.186	0.204 ± 0.010
			av	0.038	0.988 ± 0.005
	a^4F	$4s3d^8$	av	1.159	0.012 ± 0.005
	a^2F	$4s3d^8$	av	1.756	≪0.001

^{a}Statistical average over all J levels except where noted. ^{b}Energies are taken from ref 30. ^{c}Maxwell–Boltzmann distribution at 2250 ± 100 K.

TABLE II: Heats of Formation at 298 K (eV)^a

species	$\Delta_fH°$	species	$\Delta_fH°$
Co	4.42 ± 0.09	I	1.106 ± 0.0004
Co^+	12.34 ± 0.09	CH_3Cl	−0.849 ± 0.005^b
Ni	4.46 ± 0.09	CH_3Br	−0.368 ± 0.005^b
Ni^+	12.16 ± 0.09	CH_3I	0.152 ± 0.001^b
CH_3	1.51 ± 0.01	CoCl	2.00 ± 0.13
Cl	1.257 ± 0.0001	NiCl	1.89 ± 0.04
Br	1.160 ± 0.001		

^{a}All values, except where noted, are from ref 30. Ion heats of formation are calculated using the convention that the electron is a monatomic gas. Values compared from the literature which use the "stationary electron" convention should be increased by 0.064 eV at 298 K. ^{b}Pedley, J. B.; Naylor, R. D.; Kirby, S. P. *Thermochemical Data of Organic Compounds*, 2nd ed.; Chapman and Hall: London, 1986.

distribution is determined by using the octopole beam guide as a retarding potential analyzer.[14] An accurate determination is possible as the interaction region and energy analysis region are physically the same. The uncertainty in the absolute energy scale is 0.05 eV (lab). The distribution of ion energies has an average fwhm of 0.7 eV for both Co^+ and Ni^+. The thermal motion of the gas in the reaction cell contributes a large uncertainty to the collision energy.[14,15] Both effects are taken into account when the experimental results are analyzed.

Ion Source. The metal ions are produced by surface ionization (SI). In the SI source either $CoCl_2{\cdot}6H_2O$ or $NiCl_2{\cdot}6H_2O$ is dehydrated and sublimed in a resistively heated oven. The vapor is directed at a rhenium filament which is resistively heated to 2250 ± 100 K as measured by optical pyrometry. The metal complex decomposes on the filament, and metal ions are produced by surface ionization of the resulting metal atoms. If we presume that the Co and Ni reach equilibrium at the filament temperature before desorption, the electronic-state distribution of the beam produced by SI should have a Maxwell–Boltzmann distribution (Table I). Previous studies in our lab on other systems indicate that this is a reasonable approximation.[16]

We also attempted to produce a beam of pure ground-state Co^+ by using the drift cell technique described in detail in the following paper.[10] No changes in the experimental cross sections were observed for Co^+ passed through the drift cell filled with Ar or CH_4 under conditions comparable to those found to efficiently quench Fe^+ excited states. The drift cell was also filled with a mixture of CH_3I in Ar, but this completely attenuated the ion beam.

$CoCl_2{\cdot}6H_2O$ and $NiCl_2{\cdot}6H_2O$ are obtained from Mallinckrodt. CH_3Br (99.5%) is obtained from Matheson and CH_3Cl (99.5%) from Aldrich. CH_3I (99.5%) is obtained from Aldrich and is stored cold with Cu to help prevent decomposition. All of the methyl halide gases are used without further purification except for multiple freeze–pump–thaw cycles.

Thermochemical Analysis. Exothermic reaction cross sections are usually described by using the Langevin–Gioumousis–Stevensen (LGS) model[17]

$$\sigma_{\mathrm{LGS}} = \pi e(2\alpha/E)^{1/2} \tag{1}$$

where e is the electron charge, α is the polarizability of the neutral molecule, and E is the relative kinetic energy of the reactants. Many exothermic reaction cross sections follow this type of energy dependence, although deviations from this behavior are commonly seen.[18]

Cross sections for endothermic reactions can be analyzed by using eq 2

$$\sigma(E) = \sigma_0(E - E_T)^n/E^m \tag{2}$$

where E is the translational energy available to the reactants, E_T is the reaction endothermicity, σ_0 is an energy-independent scaling factor, and n and m are parameters that depend on the theoretical model being used. When the data involves a distribution of electronic states, we use

$$\sigma(E) = \sum_i g_i\sigma_{i0}(E - E_0 + E_i)^n/E^m \tag{3}$$

where we explicitly sum over the contributions of individual states, denoted by i, weighted by their populations, g_i. Here, E_0 is the threshold for reaction of the lowest electronic level of the ion and E_i is the electronic excitation of each particular J level. In the Co^+ systems, the first two electronic states (Table I) were included in the analysis with the J states for both the ^3F ground state and the ^5F first excited state resolved. In the Ni^+ systems, only the ^2D ground state (with the individual J states resolved) was included in the analysis. The $Ni^+(^4F)$ population is not included since it is quite small; see Table I. It was verified that its omission has no effect on the thermochemical results of the analysis. In the absence of information to the contrary, we assume that n, m, and σ_{i0} in eq 3 are the same for all states. Errors in threshold values are determined by the variation in E_0 for the various models applied to several data sets.

In this study, eq 3 is evaluated for the cases where $m = 0$, 1, and 3 for each endothermic reaction channel. The parameters n, σ_{i0}, and E_0 are allowed to vary freely to best fit the data as determined by nonlinear least-squares analysis. This general form and its ability to reproduce the data has been discussed previously.[19] A value of $m = 1$ is chosen because this form has been derived as a model for translationally driven reactions[20] and has been found to be quite useful in describing the shapes of endothermic reaction cross sections and in deriving accurate thermochemistry from the threshold energies, E_0, for a wide range of systems.[16,19,21,22] Data analyses that use eq 3 with $m = 0$ and $m = 3$ are included because these models provide reasonable upper and lower limits to E_0, respectively.

Heats of formation used in deriving thermochemical results are given in Table II. We assume that the neutral reactants and the products formed at the threshold of an endothermic reaction are characterized by a temperature of 298 K in all degrees of freedom. Thus, we make no correction for the energy available in internal modes of the neutral reactant. Furthermore, we implicitly assume that there are no activation barriers in excess of the endothermicity. This assumption is generally true for ion–molecule reactions and

---

(15) Chantry, P. J. *J. Chem. Phys.* **1971**, *55*, 2746–2759.

(16) Sunderlin, L. S.; Armentrout, P. B. *J. Phys. Chem.* **1988**, *92*, 1209–1219.

(17) Gioumousis, G.; Stevenson, D. P. *J. Chem. Phys.* **1958**, *29*, 292–299.

(18) Armentrout, P. B. In *Structure/Reactivity and Thermochemistry of Ions*; Ausloos, P., Lias, S. G., Eds.; Reidel: Dordrecht, 1987; pp 97–164.

(19) Aristov, N.; Armentrout, P. B. *J. Am. Chem. Soc.* **1986**, *108*, 1806–1819. Sunderlin, L. S.; Aristov, N.; Armentrout, P. B. *Ibid.* **1987**, *109*, 78–89.

(20) Chesnavich, W. J.; Bowers, M. T. *J. Phys. Chem.* **1979**, *83*, 900–905.

has been explicitly tested a number of times.[21-23] We have previously discussed the limitations on converting threshold energies, E_0, to metal ion-ligand bond energies.[19] In this study, such bond energies are measured in several systems to avoid systematic errors and the effects of activation barriers and kinetic shifts.

Results

The reactions of Co^+ and Ni^+ with CH_3X yield only two products, MCH_3^+ and MX^+ (M = Co or Ni; X = Cl, Br, or I), corresponding to reactions 4 and 5. No other products (such as

$$M^+ + CH_3X \rightarrow MCH_3^+ + X \qquad (4)$$

$$\rightarrow MX^+ + CH_3 \qquad (5)$$

MH^+, MCH_2^+, $MCHX^+$, or MCH_3X^+) were observed, although a careful search for these products was conducted. The reaction cross sections for both products formed in reactions of Ni^+ with CH_3Cl, CH_3Br, and CH_3I are shown in parts a, b, and c, respectively, of Figure 1. Parts a, b, and c of Figure 2 show comparable results for reactions of Co^+.

Metal Methyl Ion Products. When M = Ni, reaction 4 is endothermic and has a cross section that reaches a maximum of 1.0–1.5 Å^2 for all three of the methyl halides. For CH_3Cl, CH_3Br, and CH_3I, reaction 4 has an apparent threshold of ≈1.5, 1.0, and near 0.0 eV, respectively. All three of the $NiCH_3^+$ cross sections have approximately the same shape with broad peaks which continue beyond each of the neutral bond energies, $D°(CH_3\text{–}Cl) = 3.61$ eV, $D°(CH_3\text{–}Br) = 3.04$ eV, and $D°(CH_3\text{–}I) = 2.46$ eV.

Formation of $CoCH_3^+$ is endothermic for both CH_3Cl and CH_3Br. The reactions have apparent thresholds of about 1.5 and 0.5 eV, respectively. Both product cross sections reach maxima of about 1.0 Å^2, about 1.0 eV above the respective neutral bond energies. Beyond these maxima, the cross sections decrease, presumably due to dissociation to $Co^+ + CH_3 + X$.

The $CoCH_3^+$ cross section from the reaction of Co^+ with CH_3I has quite unusual behavior; see Figure 2c. At low energies, the reaction is clearly exothermic, with the cross section decreasing approximately as $(0.16 \pm 0.06)\sigma_{LGS}$, but then as $E^{-1.6\pm0.1}$ above about 0.3 eV. At still higher energies, the cross section levels out until about 8 eV, before decreasing at energies well above $D°(CH_3\text{–}I)$. This high energy behavior is similar to that of $\sigma(CoCH_3^+)$ from both methyl chloride and methyl bromide.

Metal Halide Ion Products. The $NiCl^+$ product cross section shown in Figure 1a looks very much like the $NiCH_3^+$ cross section for the $Ni^+ + CH_3Cl$ reaction, although its apparent threshold at about 1.2 eV is slightly less than that for $NiCH_3^+$. Production of $CoCl^+$ is only slightly endothermic, with an apparent threshold of about 0.4 eV, and has two features as can be seen in Figure 2a. The bimodal behavior exhibited by the $CoCl^+$ cross section suggests the possibility of two reaction mechanisms for the formation of this product. The most notable difference between the two $M^+ + CH_3Cl$ systems is that the two features seen in the $CoCl^+$ product cross section are not seen in $\sigma(NiCl^+)$.

The cross section for $NiBr^+$ has two features (Figure 1b): an exothermic portion below 0.7 eV, decreasing as $E^{-1.1\pm0.1}$, and one that has an apparent onset of about 0.8 eV. Much like $\sigma(NiBr^+)$, the $CoBr^+$ product cross section is exothermic at low energies, decreasing as $E^{-0.85\pm0.1}$, but has a second feature arising at about 2 eV (Figure 2b).

The NiI^+ product cross section also has two features (Figure 1c). At very low energies, formation of NiI^+ is exothermic, with the cross section decreasing at the lowest energies as about $0.2\sigma_{LGS}$, then as $E^{-1.2\pm0.1}$ above about 0.3 eV. In the reaction of Co^+ with CH_3I, the CoI^+ cross section is similar to that of the $CoCH_3^+$ in

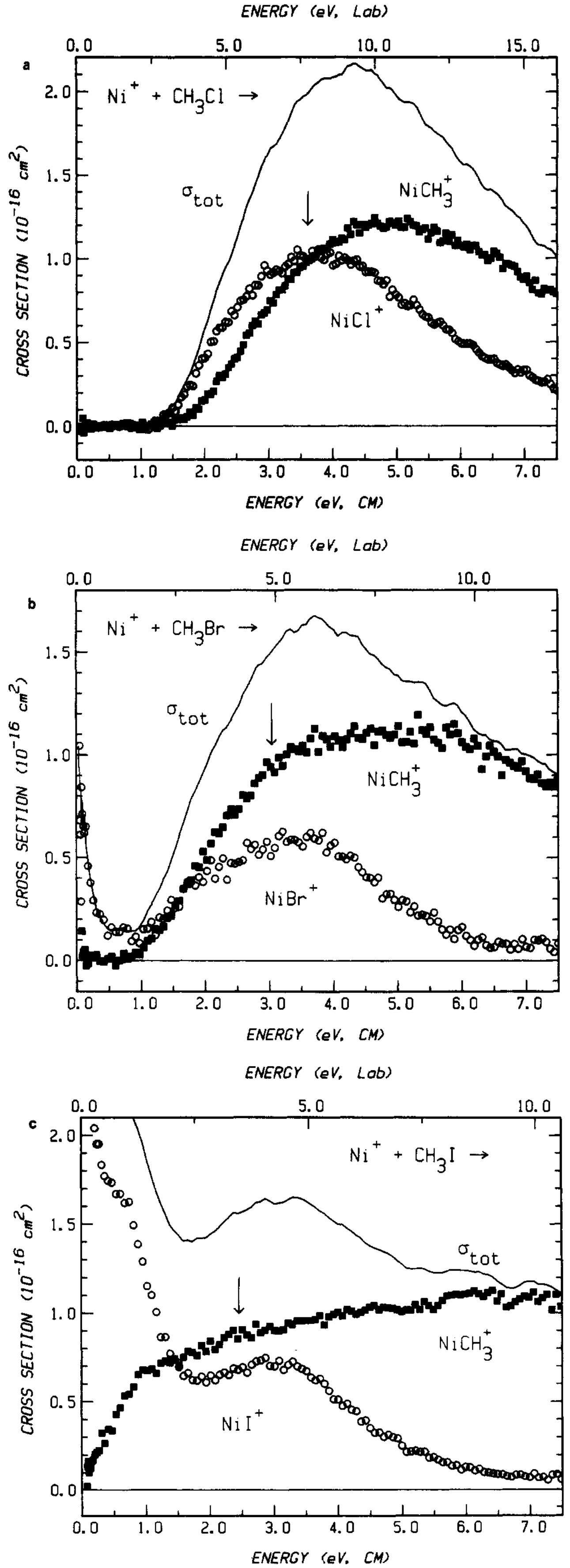

Figure 1. Variation of product cross sections with translational energy in the laboratory frame of reference (upper scale) and the center-of-mass frame (lower scale) for reaction of Ni^+ with CH_3Cl (part a), with CH_3Br (part b), and with CH_3I (part c). The solid lines represent the smoothed total cross section for reactions 4 and 5. The arrows represent $D°(CH_3\text{–}X)$.

---

[21] Boo, B. H.; Armentrout, P. B. *J. Am. Chem. Soc.* **1987**, *109*, 3549–3559.

[22] Weber, M. E.; Armentrout, P. B. *J. Chem. Phys.* **1988**, *88*, 6898–6910.

[23] Ervin, K. M.; Armentrout, P. B. *J. Chem. Phys.* **1986**, *84*, 6738–6749. Boo, B. H.; Armentrout, P. B. *J. Am. Chem. Soc.* **1987**, *109*, 3549–3559. Ervin, K. M.; Armentrout, P. B. *J. Chem. Phys.* **1987**, *86*, 2659–2673. Elkind, J. L.; Armentrout, P. B. *J. Phys. Chem.* **1984**, *88*, 5454–5456.

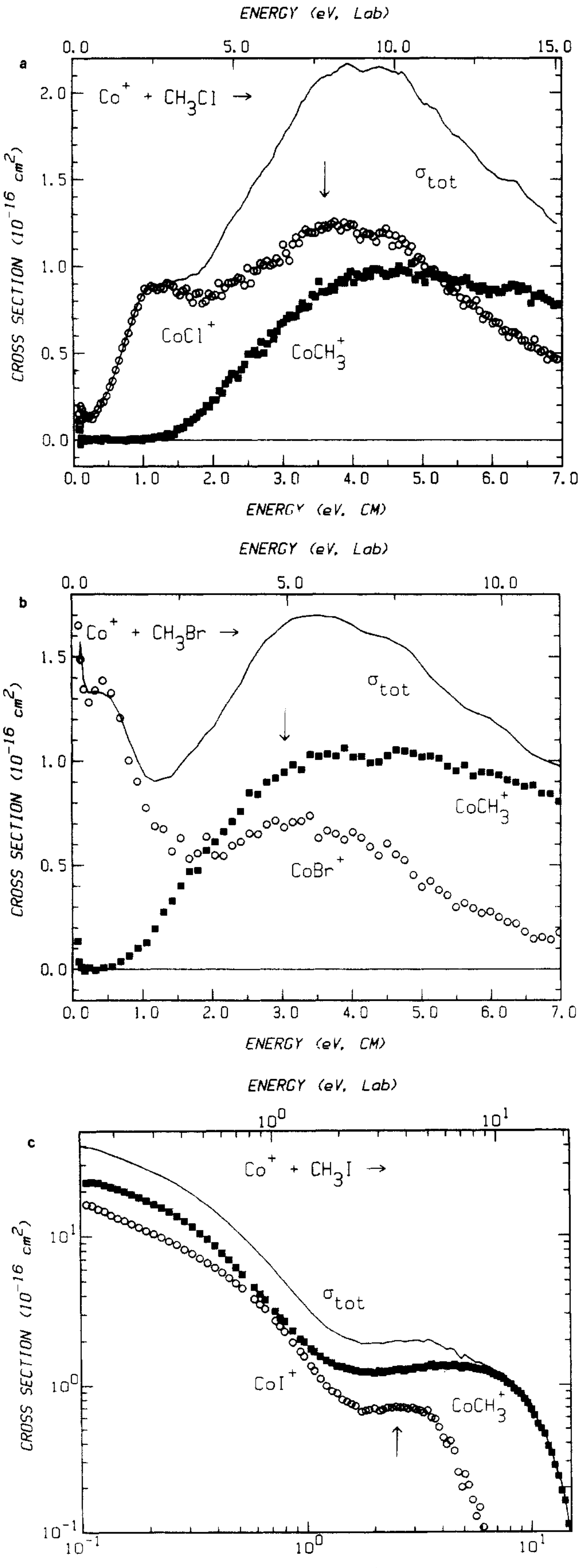

Figure 2. Variation of product cross sections with translational energy in the laboratory frame of reference (upper scale) and the center-of-mass frame (lower scale) for reaction of Co^+ with CH_3Cl (part a), with CH_3Br (part b), and with CH_3I (part c). The solid lines represent the smoothed total cross section for reactions 4 and 5. The arrows indicate $D°(CH_3–X)$.

TABLE III: Optimum Parameters for Threshold Fits[a]

reaction products	n	σ_{i0}	E_0, eV	av E_0,[b] eV
$NiCH_3^+ + Cl$	1.4 ± 0.20	1.9 ± 0.3	1.80 ± 0.06	1.82 ± 0.06
$NiCH_3^+ + Br$	1.5 ± 0.18	0.8 ± 0.2	1.08 ± 0.19	1.06 ± 0.17
$NiCH_3^+ + I$	1.2 ± 0.08	1.0 ± 0.4	0.32 ± 0.08	0.32 ± 0.08
$CoCH_3^+ + Cl$	1.2 ± 0.05	1.3 ± 0.1	1.72 ± 0.06	1.70 ± 0.14
$CoCH_3^+ + Br$	1.6 ± 0.18	0.9 ± 0.1	0.81 ± 0.06	0.81 ± 0.06
$CoCH_3^+ + I$	1.8 ± 0.15	0.7 ± 0.1	0.25 ± 0.05	0.25 ± 0.05
$NiCl^+ + CH_3$	1.0 ± 0.15	1.9 ± 0.3	1.55 ± 0.02	1.56 ± 0.04
$CoCl^+ + CH_3$	1.0 ± 0.23	1.8 ± 0.2	0.68 ± 0.06	0.57 ± 0.12

[a] Optimum value of parameters in eq 3 when $m = 1$. [b] Average value for all threshold analyses including forms where m = 0, 1, and 3, except for CH_3I systems where only $m = 1$ fits reproduced the data.

both size and shape. The low-energy feature of $\sigma(CoI^+)$, however, is smaller than $\sigma(CoCH_3^+)$, and at higher energies, the cross section decreases earlier than $\sigma(CoCH_3^+)$.

Comparison to Previous Results. When AR studied the reaction of Ni^+ with CH_3I, and CH_3Br at thermal energies, they did not observe $NiCH_3^+$. This is in agreement with the results reported here. With Co^+, AR found the branching ratio between $CoCH_3^+$ and CoI^+ in the reaction with CH_3I to be 27:73[1] and, on the basis of reported reaction rates, 42:58.[2] We determine a branching ratio between the two product channels of 60:40 ± 5. This discrepancy may originate from different electronic-state populations of Co^+ in AR's and our experiments. When we examined the reaction of CH_3I with Co^+ formed by electron impact (Ee ~ 50 eV) on $Co_2(CO)_8$ (conditions that are known to produce excited states),[8] the branching ratio between $CoCH_3^+$ and CoI^+ was indeed altered slightly to about 40:60, in better agreement with AR's result. It is, therefore, possible for the apparent branching ratio to shift with different ion state populations.

In addition to branching ratios, AR report a total reaction rate of 1.9×10^{-10} cm^3 mol^{-1} s^{-1} for reactions 4 and 5 with M = Co and X = I.[2] The reaction rate derived here for the same reaction is $(2.7 \pm 0.6) \times 10^{-10}$ cm^3 mol^{-1} s^{-1}. Again this discrepancy between our results and AR's may originate from the differences in excited-state populations in the two experiments, but the values are probably within experimental error. AR did not report reaction rate values for the reaction of CH_3Br with Co^+ and the analogous Ni^+ reactions. We derive rates of $(2.3 \pm 0.46) \times 10^{-11}$ cm^3 mol^{-1} s^{-1} for the $Co^+ + CH_3Br$ reaction, $(5.0 \pm 1.0) \times 10^{-12}$ cm^3 mol^{-1} s^{-1} for $Ni^+ + CH_3Br$, and $(2.0 \pm 0.4) \times 10^{-11}$ cm^3 mol^{-1} s^{-1} for reaction of Ni^+ with CH_3I.

Thermochemistry

Reactions 4 and 5 for each system are analyzed by using eq 3 as discussed above. Detailed results for the $m = 1$ optimized fits to the data are given in Table III for all endothermic reactions. With two exceptions, the average E_0 values cited are the average threshold energies for the m = 0, 1, and 3 analyses. The error reported is the pooled estimate of error.[24] For reaction 4 with M = Ni and X = I, the reaction cross sections could only be reproduced when $m = 1$. For reaction 4 with M = Co and X = I, analysis of the $CoCH_3^+$ cross section was not straightforward and will be discussed below. The errors in E_0 cited in these cases arise from variations in different data sets and different values of n. The thermochemical results of these analyses are discussed below.

$NiCH_3^+$. In all three nickel systems, the formation of $NiCH_3^+$ is endothermic. Figure 3 shows typical threshold analyses of reaction 4 for all three methyl halides. It can be seen that the data is reproduced very well by using eq 3 with the parameters of Table III. Using the average thresholds for reaction 4 given in Table III and the bond energies for CH_3X calculated from information in Table II [$D°(CH_3–Cl) = 3.61 \pm 0.02$ eV, $D°(CH_3–Br) = 3.04 \pm 0.01$ eV, and $D°(CH_3–I) = 2.46 \pm 0.02$ eV],

---

[24] Box, G. E. P.; Hunter, W. G.; Hunter, J. S. *Statistics for Experimenters*; Wiley: New York, 1978; p 319.

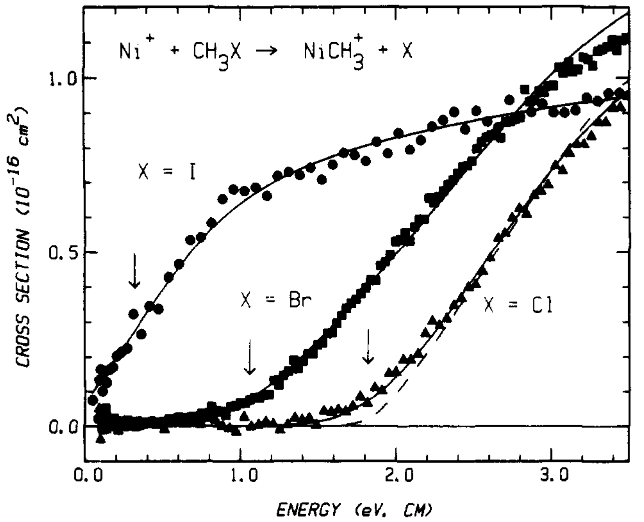

Figure 3. Threshold region of reaction 4 with M = Ni and X = Cl, Br, and I. Arrows indicate the threshold for the three reactions at 1.82, 1.06, and 0.32 eV, respectively. The solid lines show the threshold fits calculated by using eq 3 and the parameters given in Table III. The dashed line shows the unconvoluted cross section for the reaction of Ni^+ with CH_3Cl.

TABLE IV: Bond Dissociation Energies (eV)

system	$D°(M^+–CH_3)$	$D°(M^+–X)$
Ni^+:CH_3Cl	1.79 ± 0.06	2.05 ± 0.10
Ni^+:CH_3Br	1.98 ± 0.17	>3.04
Ni^+:CH_3I	2.14 ± 0.08	>2.46
Ni^+:ethane[a]	1.95 ± 0.10	
average	1.96 ± 0.13	
Co^+:CH_3Cl	1.91 ± 0.14	3.04 ± 0.12
Co^+:CH_3Br	2.23 ± 0.06	>3.04
Co^+:CH_3I	2.21 ± 0.05	>2.46
Co^+:ethane[a]	2.13 ± 0.15	
average	2.12 ± 0.13	

[a] Values from ref 6.

we obtain the $Ni^+–CH_3$ bond energies at 298 K that are listed in Table IV. These values can be favorably compared with that derived from the reaction of Ni^+ with ethane, 1.95 ± 0.10 eV.[6]

$CoCH_3^+$. Shown in Figure 4 is a threshold analysis of the reaction of $Co^+ + CH_3Br \rightarrow CoCH_3^+ + Br$ using eq 3 and the parameters of Table III. The calculated cross sections for the deconvolution of the cross section into ground- and excited-state processes are also shown. Contributions from the $Co^+(^5F)$ first excited state (which has a 16% population; Table I) are clearly appreciable. If both states react efficiently, reliable analysis of the endothermic reactions of Co^+ with the methyl halides requires the use of eq 3 rather than eq 2. We find that the cross sections for reaction 7 for the CH_3Cl and CH_3Br systems can *only* be reproduced when eq 3 and both electronic states are included. The single state eq 2 is inadequate. Thus, *both the ^3F and ^5F states appear to react with the methyl halides with comparable efficiencies.*

The values for $D°(Co^+–CH_3)$ derived from the CH_3Cl and CH_3Br data are consistent with that found for the reaction of Co^+ with ethane; see Table IV. These bond energies indicate that the reaction of $Co^+ + CH_3I \rightarrow CoCH_3^+ + I$ should be endothermic by about 0.3 eV. At first, this appears to conflict with the data of Figure 2c which clearly indicate that the formation of $CoCH_3^+$ from this reaction has an exothermic component. However, since we believe that $Co^+(^5F)$ reacts efficiently with the methyl halides, we propose that the exothermic reactivity exhibited by the $CoCH_3^+$ cross section is due to the reaction of this excited state of Co^+. Even the lowest *J* component of this state has sufficient electronic energy (Table I) to overcome the 0.3-eV endothermicity of the reaction. This proposal is made more plausible by the observation of the plateau region in the $CoCH_3^+$ cross section, since this can now be attributed to the endothermic reaction of the $Co^+(^3F)$ ground state. Reaction of both the ground state and first excited state of cobalt with the other two methyl halides is sufficiently endothermic that no exothermic behavior would be present in these systems.

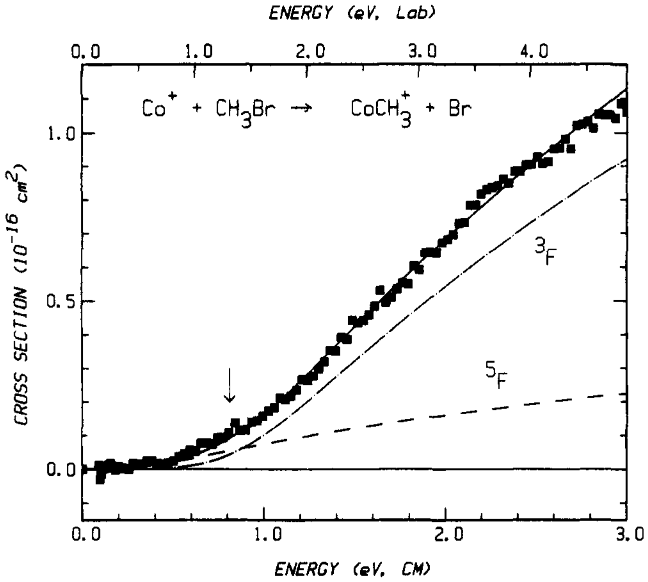

Figure 4. Threshold region of reaction 4 with M = Co and X = Br. The solid line shows the threshold fit calculated by using eq 3 with the parameters of Table III. The dashed line shows the cross section attributed to reaction of $Co^+(^5F)$, and the dash–dot line shows the contribution of the $Co^+(^3F)$ ground-state reaction.

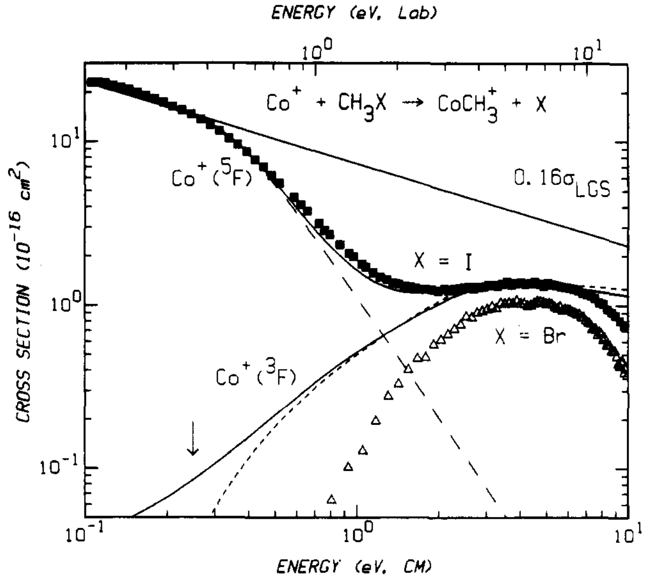

Figure 5. Threshold analysis of the reaction of Co^+ with CH_3I to form $CoCH_3^+$. The upper solid line shows $0.16\sigma_{LGS}$. Other lines show the calculated cross sections for the postulated deconvolution of the cross section into the $Co^+(^3F)$ ground-state and $Co^+(^5F)$ excited-state processes. The unconvoluted $Co^+(^3F)$ cross section is shown by a dashed line. The derived threshold energy for this process is denoted by the arrow at 0.25 eV. The convoluted ^3F (lower solid line) and ^5F (long dashed line) calculations are summed to give the solid line running through the data points (solid squares) for $\sigma(CoCH_3^+)$. The open triangles are the $CoCH_3^+$ cross section from the reaction of Co^+ with CH_3Br.

To further confirm this hypothesis, we have analyzed the $CoCH_3^+$ cross section in detail. At the very lowest energies, the cross section can be described by using $0.155\sigma_{LGS}$, Figure 5. This fraction is in excellent agreement with the expected population of the $Co^+(^5F)$ state, 16 ± 1% at the filament temperature used; see Table I. This correlation helps validate the assignment of the low-energy reaction to the $Co^+(^5F)$ excited state and further suggests that this state reacts with near unit efficiency.[25] At slightly higher energies, $\sigma(\mathrm{CoCH_3^+})$ begins to decline faster than σ_{LGS}. We have seen this type of falloff in other systems and have attributed this behavior to angular momentum constraints. As discussed in detail elsewhere,[26] it is possible to calculate the energy where the deviation from σ_{LGS} should begin. Here we calculate that this deviation should occur at 0.42 ± 0.24 eV, compared with the data which show a deviation from σ_{LGS} at 0.33 eV (Figure 5).

After having accounted for the low-energy feature in the data, we are then able to model the high-energy feature of $\sigma(\mathrm{CoCH_3^+})$. The "endothermic" portion of the $\mathrm{CoCH_3^+}$ cross section is remarkably similar in both size and shape to $\sigma(\mathrm{CoCH_3^+})$ from $\mathrm{Co^+} + \mathrm{CH_3Br}$ (Figure 5). Therefore, it is possible to successfully model the high-energy behavior by using the same n and m values in eq 4 that were used to interpret the $\mathrm{CH_3Br}$ data and by adjusting E_0 to account for the difference between $D°(\mathrm{CH_3{-}Br})$ and $D°(\mathrm{CH_3{-}I})$. If E_0 is then allowed to optimize, this analysis yields a threshold energy of 0.25 ± 0.05 eV for the formation of $\mathrm{CoCH_3^+}$ from ground-state $\mathrm{Co^+(^3F)}$. This yields a value for $D°(\mathrm{Co^+{-}CH_3})$ (Table IV) that is consistent with all the others. The low-energy fit, high-energy fit, and their sum are compared with $\sigma(\mathrm{CoCH_3^+})$ from the reaction of $\mathrm{Co^+}$ with $\mathrm{CH_3I}$ in Figure 5. The agreement between the data and the sum of the high- and low-energy fits is excellent.

Comparison to Previous Values. The bond energies derived here for the ionic metal–methyl bonds are in good agreement with those derived from the ethane studies.[6] If the three bond energy values derived here for each system are averaged with the analogous ethane results, the resulting value is almost exactly equal to the value derived directly from the ethane reaction for both metals; see Table IV. Also, if comparison between metal systems is made for each neutral molecule ($\mathrm{C_2H_6}$, $\mathrm{CH_3Cl}$, $\mathrm{CH_3Br}$, and $\mathrm{CH_3I}$), the average difference in bond energies is nearly invariable; $D°(\mathrm{Co^+{-}CH_3}) - D°(\mathrm{Ni^+{-}CH_3}) = 0.18 \pm 0.05$ eV. Although there may be systematic differences in the bond dissociation energies derived from some of the neutral molecules (e.g., $\mathrm{CH_3Cl}$), these differences are the same, regardless of the metal ion. We therefore recommend the values derived from the most recent ethane studies for the ionic metal methyl bond strengths; $D°(\mathrm{Co^+{-}CH_3}) = 2.13 \pm 0.15$ eV and $D°(\mathrm{Ni^+{-}CH_3}) = 1.95 \pm 0.10$ eV.[6]

These results not only are consistent with our previous thermochemical studies, but they allow us to understand the discrepancy with the results of Allison and Ridge (AR). As noted in the Introduction, AR found that $\mathrm{NiCH_3^+}$ was not formed at thermal energy with any of the methyl halides while $\mathrm{CoCH_3^+}$ was formed at thermal energy in the reaction with methyl iodide. These results are in complete agreement with the experiments reported here. AR made the reasonable conclusion that $D°(\mathrm{Ni^+{-}CH_3}) < 2.46\ \mathrm{eV} = D°(\mathrm{CH_3{-}I})$ and that $2.46\ \mathrm{eV} < D°(\mathrm{Co^+{-}CH_3}) < 3.04\ \mathrm{eV} = D°(\mathrm{CH_3{-}Br})$. Our results show, however, that the exothermic reaction of $\mathrm{Co^+}$ with $\mathrm{CH_3I}$ is due to the $\mathrm{Co^+(^5F)}$ excited state. This means that $D°(\mathrm{Co^+{-}CH_3}) > 2.46\ \mathrm{eV} - E_{\mathrm{el}}(^5\mathrm{F}) \approx 2.0$ eV, in agreement with the present results. AR produced $\mathrm{Co^+}$ by electron impact (EI) on $\mathrm{Co(CO)_3NO}$. Although AR note that the measured reaction rates are not dependent on the energy of the ionizing electrons, work in our laboratory has shown evidence of excited states from EI ionization of $\mathrm{Co_2(CO)_8}$ (at 50 eV).[8]

In previous ion beam studies of the reactions of $\mathrm{Co^+}$ and $\mathrm{Ni^+}$ with ethane, the bond energies $D°(\mathrm{Co^+{-}CH_3}) = 2.64 \pm 0.2$ eV[5] and $D°(\mathrm{Ni^+{-}CH_3}) = 2.08 \pm 0.22$ eV[27] were determined. While the latter value agrees with that determined here, the former is substantially different. As discussed in detail elsewhere,[6] the results reported by Armentrout and Beauchamp for the $\mathrm{Co^+{-}CH_3}$ bond energy do not result from qualitatively different data but arise from different interpretation of the reaction thresholds. The early data were not sufficiently precise to unambiguously determine the threshold without constraining the number of freely varying parameters. With the improved ion beam technology currently available, this constraint has been largely removed.

There exist two other determinations of the $\mathrm{Co^+}$–methyl bond strength. Freiser and co-workers have reported $D°(\mathrm{Co^+{-}CH_3}) = 2.5 \pm 0.3$ eV[28] from photoionization studies of $\mathrm{CoCH_3^+}$ and $D°(\mathrm{Co^+{-}CH_3}) = 2.0 \pm 0.6$ eV[29] from a study of the reactions of $\mathrm{Co^+}$ with ethane. Both of these values are in reasonable agreement with those determined here and by Georgiadis, Fisher, and Armentrout.[6]

$\mathrm{MX^+}$ Thermochemistry. The only metal halide products formed by endothermic processes in these reactions are the $\mathrm{MCl^+}$ ions. Representative analyses of the $\mathrm{CoCl^+}$ and $\mathrm{NiCl^+}$ products are listed in Table III. The reaction thresholds are converted to the bond energies $D°(\mathrm{Co^+{-}Cl}) = 3.04 \pm 0.12$ eV and $D°(\mathrm{Ni^+{-}Cl}) = 2.05 \pm 0.10$ eV. Since all of the other $\mathrm{MX^+}$ ions are products of exothermic reactions, we can only place lower limits on their bond strengths (Table IV).

Information on the ionization potential (IP) of the metal chlorides can be obtained by the use of eq 6. From our value

$$\mathrm{IP(MCl)} = D°(\mathrm{M{-}Cl}) + \mathrm{IP(M)} - D°(\mathrm{M^+{-}Cl}) \qquad (6)$$

for $D°(\mathrm{Co^+{-}Cl})$, $D°(\mathrm{Co{-}Cl}) = 3.68 \pm 0.13$ eV, and $\mathrm{IP(Co)} = 7.86 \pm 0.01$ eV,[30] we are able to derive $\mathrm{IP(CoCl)} = 8.5 \pm 0.2$ eV. This seems reasonable since it is close to IP(Co) and is much lower than $\mathrm{IP(Cl)} = 12.97$ eV.[29] A similar treatment for NiCl, where $D°(\mathrm{NiCl}) = 3.83 \pm 0.04$ eV[29] and $\mathrm{IP(Ni)} = 7.638 \pm 0.001$ eV,[30] gives $\mathrm{IP(ICl)} = 9.4 \pm 0.1$ eV. This is much lower than a value cited in the literature, $\mathrm{IP(NiCl)} = 11.4 \pm 0.2$ eV,[31] but this IP would mean that $D°(\mathrm{Ni^+{-}Cl}) = 0.05$ eV. This is clearly inconsistent with the data of Figure 1a and much too low to be plausible.

The values for the neutral and ionic metal chloride bond energies are in agreement with limits inferred by Allison and Ridge.[3] They observed that reaction 7 occurred at thermal energies for both Co and Ni while reaction 8 did not. These observations suggest

$$\mathrm{M^+} + 2\text{-}\mathrm{C_3H_7Cl} \rightarrow \mathrm{MCl} + 2\text{-}\mathrm{C_3H_7^+} \qquad (7)$$

$$\rightarrow \mathrm{MCl^+} + 2\text{-}\mathrm{C_3H_7} \qquad (8)$$

that $D°(\mathrm{M^+{-}Cl}) < 3.63\ \mathrm{eV} = D°(2\text{-}\mathrm{C_3H_7{-}Cl})$[32] for both $\mathrm{Co^+}$ and $\mathrm{Ni^+}$, which agrees with the specific values derived here (Table IV). In addition, the fact that reaction 7 is observed must mean that $\mathrm{IP(MCl)} > \mathrm{IP}(2\text{-}\mathrm{C_3H_7}) = 7.36$ eV,[33] again in agreement with the specific IP(MCl) values derived here.

$\mathrm{MX^+}$ Bonding. An interesting detail about the $\mathrm{MCl^+}$ products is their bonding characteristics which can be understood by considering a simple description employed by Mandich, Steigerwald, and Reents (MSR).[34] MSR have studied the reactions of $\mathrm{ClCr^+}$, $\mathrm{ClMn^+}$, and $\mathrm{ClFe^+}$ with small alkanes via Fourier transform ICR. They found that while $\mathrm{ClCr^+}$ was very reactive with small alkanes, $\mathrm{ClMn^+}$ and $\mathrm{ClFe^+}$ were not nearly as reactive. They also examined the bonding between the chlorine ligand and the metal ions with the use of ab initio calculations. According to MSR, one view of the metal–chlorine bonding is that it is ionic,

---

(25) This comparison is probably more complicated. First, the ^{5}F state presumably forms $\mathrm{CoI^+}$ as well as $\mathrm{CoCH_3^+}$. This would mean that the apparent population of the ^{5}F is higher than 16%. Second, the true collision cross section is probably higher than the LGS limit for these reactions due to the strong ion–dipole attraction. This is discussed in detail in ref 10 where deviations from LGS are observed for reaction of $\mathrm{Fe^+(^4F)}$ with the methyl halides. This consideration lowers the apparent $\mathrm{Co^+(^5F)}$ population. Thus, these two effects may cancel one another.

(26) Burley, J. D.; Ervin, K. M.; Armentrout, P. B. *Int. J. Mass Spectrom. Ion Processes* **1987**, *80*, 153–175.

(27) Halle, L. F.; Armentrout, P. B.; Beauchamp, J. L. *Organometallics* **1982**, *1*, 963–968.

(28) Hettich, R. L.; Jackson, T. C.; Stanko, E. M.; Freiser, B. S. *J. Am. Chem. Soc.* **1986**, *108*, 5086–5093.

(29) Forbes, R. A.; Lech, L. M.; Freiser, B. S. *Int. J. Mass Spectrom. Ion Processes* **1987**, *77*, 107–121.

(30) Sugar, J.; Corliss, C. *J. Phys. Chem. Ref. Data* **1985**, *14*, Suppl. 2.

(31) McKinley, J. D. *J. Chem. Phys.* **1964**, *40*, 120–125.

(32) Derived from heats of formation found in ref 30 and in Pedley, J. B.; Naylor, R. D.; Kirby, S. P. *Thermochemical Data of Organic Compounds*, 2nd ed.; Chapman and Hall: London, 1986.

(33) Schultz, J. C.; Houle, F. A.; Beauchamp, J. L. *J. Am. Chem. Soc.* **1984**, *106*, 3917–3927.

(34) Mandich, M. L.; Steigerwald, M. L. Reents, W. D., Jr. *J. Am. Chem. Soc.* **1986**, *108*, 6197–6202.

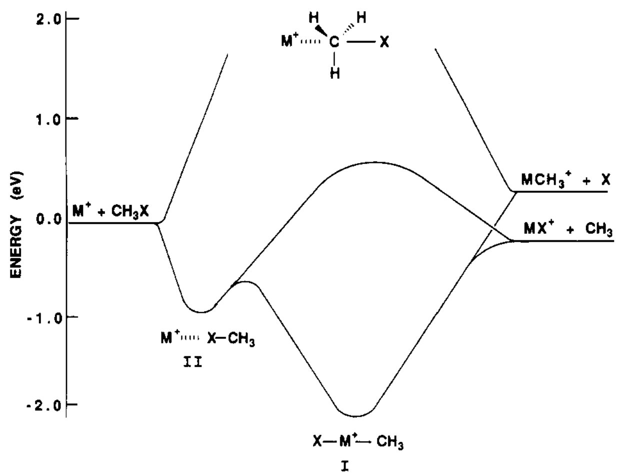

Figure 6. Qualitative potential energy surfaces for interaction of M^+ with the methyl halides.

due to the large difference in electronegativity between Cl and the transition metals. Qualitatively, the neutral ClM becomes Cl^-–M^+, and ClM^+ becomes Cl^-–M^{2+}. For the metals studied by MSR, this bonding picture is in accord with their calculations for the neutral species. They also concluded that ionic bonding does not appear to be an important factor in the bonding scheme for $ClMn^+$ or $ClFe^+$ but does describe the bonding in $ClCr^+$. This explains the difference in reactivity between the metal halogen species. These results are also in agreement with recent ab initio calculations of the electronic and geometric structure for $ClCr^+$ by Alvarado-Swaisgood and Harrison.[35]

In the cases of Co and Ni, qualitative calculations comparable to those done by MSR can be made to determine the nature of the MCl^+ bond. These reveal that the M^+–Cl bond appears to be primarily covalent for these metals, similar to Fe and Mn. Likewise these ideas suggest that CoCl and NiCl have primarily ionic bonding. This difference in bonding character may explain why $D°$(M–Cl) is stronger than $D°$(M^+–Cl).

Reaction Mechanism

The reactions of Co^+ and Ni^+ with the methyl halides are most easily explained by the previously proposed mechanism,[3] i.e., insertion of the metal into the C–X bond to form the intermediate I, CH_3–M^+–X. The failure to observe MH^+ in both metal systems (which could result from a competitive C–H bond insertion mechanism) can be rationalized because the C–X bond is weaker than the C–H bond and $D°$(M^+–X) is stronger than $D°$(M^+–H).

Insight into the dynamics and reaction mechanisms of the methyl halide systems can be obtained by constructing potential energy surfaces (PESs). The following treatment is only semiquantitative but is designed to elucidate the important qualitative features in these reactions. As M^+ and the methyl halide approach, there is a long-range attraction due to the ion dipole potential; see Figure 6. In the most favorable configuration, the dipole "locks" onto the ion, and M^+···X–CH_3, intermediate II, is formed. At a reasonable distance of approach (~2.3 Å), this species is about 1 eV more stable than the reactants for all three methyl halides. If M^+ approaches the carbon end of CH_3X, the long-range interaction is repulsive due to the unfavorable dipole orientation. From II, intermediate I can be formed via C–X bond insertion of the metal ion. While no direct experimental information is available concerning the thermochemical stability of I, we can estimate this by assuming that the bond energies in I are the same as for singly ligated M^+. This bond additivity assumption is not necessarily quantitative but is probably sufficiently accurate to identify the general reactivity trends. On the basis of these arguments, intermediate I lies in a well that is 1.5–2.2 eV deep and thus is not expected to have a barrier to formation for any of the reactions. The subsequent loss of either X or CH_3 from this intermediate would account for the two products formed in each system.

Intermediate I clearly can explain how both MCH_3^+ and MX^+ are formed but fails to account for the dual features in the MX^+ cross sections. In analogy with our analysis for $CoCH_3^+$ from CH_3I, we might have explained the two features in all three CoX^+ cross sections, Figure 2a–c, as due to the presence of excited state ions. However, similar behavior is also observed in the $NiBr^+$ and NiI^+ cross sections, Figure 1b,c, and here it is not possible for the large low-energy features to be produced by excited-state nickel ions. This is because Ni^+(SI) comprises <2% ground-state ions, Table I, while the low-energy features have magnitudes which are greater than 2% of σ_{LGS}. Further, in our companion study of the state-specific reactions of $Fe^+(^6D)$ and $Fe^+(^4F)$,[10] we again see two features in the FeX^+ cross sections, but these appear for *both* electronic states. Thus, the $\sigma(MX^+)$ features cannot be explained by reactions of different electronic states.

We propose, instead, that the behavior exhibited by the MX^+ cross sections is due to different reaction mechanisms. At low energies, the MX^+ product is formed from the intermediate complex I in the metal insertion mechanism. This is the most efficient process at low energies and proceeds with little or no barrier. The formation of MX^+ at higher energies, evidenced by the second feature in the MX^+ cross section, could be explained by a direct interaction between the metal ion and the halogen atom on the methyl halide. One way to think about this direct interaction is to view the reaction in reverse, i.e., CH_3 approaching MX^+. If CH_3 approaches the metal end of MX^+, a covalent bond can be formed and intermediate I is generated. However, if CH_3 approaches the halide end, there are no unpaired electrons available for bonding on the halide such that the interaction is anticipated to be much more repulsive. Eventually, however, this interaction should lead directly to intermediate II. This surface is shown in Figure 6. A comparable duplicity in interactions can occur for MCH_3^+ + X, but now the MCH_3^+···X approach leads to the M^+···CH_3–X reactant approach. Because this interaction is very repulsive, no secondary features are observed in the MCH_3^+ cross sections.

A somewhat different perspective on these reactions (in particular, Co^+ + CH_3I) has been forwarded by Allison, Mavridis, and Harrison.[36] These authors discuss the significance of spin conservation in this reaction and conclude that the insertion mechanism might involve a large activation barrier since it could involve mixing of a high-energy triplet $Co^+(4s3d^7)$ configuration. While there is insufficient experimental or theoretical evidence to determine this definitively one way or another, we believe that the necessary orbital mixing does not lead to an activation barrier. We base this conclusion on our past work on the reactions of various electronic states of transition metals with H_2 and alkanes.[6,9]

One final feature of the present results is that both the $^5F(4s3d^7)$ excited state and the $^3F(3d^8)$ ground state of Co^+ appear to react efficiently with the methyl halides. In contrast there is no clear evidence for reactivity of $Co^+(^5F)$ with H_2 and alkanes.[6,9] This situation is directly analogous to results for the $^6D(4s3d^6)$ ground state and the $^4F(3d^7)$ excited state of Fe^+. This is discussed in the following paper, which details these results for iron,[10] but it seems clear that the interactions of the metal ions with the polar methyl halide molecules enable more efficient mixing of different spin states than is achieved in the interactions with small saturated hydrocarbons.[37,38] For larger, more polarizable hydrocarbons,

---

[35] Alvarado-Swaisgood, A. E.; Harrison, J. F. *J. Phys. Chem.* **1988**, *92*, 5896–5900.

[36] Allison, J.; Mavridis, A.; Harrison, J. F. *Polyhedron* **1988**, *7*, 1559–1572.

[37] Similar considerations explain why collisional relaxation of Co^+ excited states with Ar or CH_4 is much less efficient for Fe^+ excited states. In this regard, we note that the surfaces correlating to $Fe^+(^4F,3d^7)$ are more attractive than the relatively repulsive $Fe^+(^6D,4s3d^6)$ surfaces. Thus, these surfaces probably cross as the reactants approach, as shown in a recent publication for the interaction of Fe^+ with Ar.[38] In contrast, on the basis of the electron configurations of the analogous states, we expect that the $Co^+(a^3F,3d^8)$ ground-state surfaces should be more attractive than the $Co^+(^5F,4s3d^7)$ excited-state surfaces. Thus, these surfaces probably cross at an elevated potential energy making collisional cooling difficult under thermal conditions.

J. Phys. Chem. 1989, 93, 7382–7387

however, such mixing has been postulated in the reactions of Fe^+.[9]

Summary

The reactions of Co^+ and Ni^+ with CH_3X (X = Cl, Br, or I) are studied by using guided ion beam mass spectrometry. In all reactions, only two ionic products are observed, MX^+ and MCH_3^+. $D°(M^+–CH_3)$ values for M = Co and Ni are derived in each of the systems. These bond strengths agree well with our earlier determinations from alkane studies, but the $CoCH_3^+$ bond energy conflicts with other literature values. In addition, M^+–Cl bond energies are determined for both metals from the reaction with CH_3Cl. Previous values for the MCl^+ bond strengths are not available for comparison. The IP(NiCl) value determined here, however, differs by >2 eV from an earlier reported value which is clearly in error.

The reaction of $Co^+ + CH_3I$ forms $CoCH_3^+$ via both an exothermic and endothermic pathway. We explain this as due to electronic state effects; i.e., the $Co^+(^5F)$ first excited state reacts very efficiently and exothermically with methyl iodide, while the $Co^+(^3F)$ ground state reacts endothermically. This behavior is successfully modeled here and explains why we reach different thermochemical conclusions for $D°(Co^+–CH_3)$ than those obtained by Allison and Ridge from ICR studies of the same reactions.[1–3]

Two reaction mechanisms are proposed that explain dual features seen in the formation of MX^+. At low energies, an intermediate complex is formed by insertion of the metal ion into the C–X bond of CH_3X. This then leads to MCH_3^+ and MX^+ formation. At high energies, a direct mechanism in which the incident ion interacts primarily with the halide atom accounts for a second feature in the MX^+ cross section.

Acknowledgment. This work was funded by the National Science Foundation, Grant CHE-8796289. E.R.F. thanks David A. Hales and Dr. Mary Ellen Weber for their help in performing these experiments.

Registry No. Co^+, 16610-75-6; Ni^+, 14903-34-5; CH_3Cl, 74-87-3; CH_3Br, 74-83-9; CH_3I, 74-88-4.

---

(38) Loh, S. K.; Fisher, E. R.; Lian, L.; Schultz, R. H.; Armentrout, P. B. *J. Phys. Chem.* **1989**, *93*, 3159–3167.

Guided Ion Beam Studies of the State-Specific Reactions of $Fe^+(^6D,^4F)$ with CH_3X (X = Cl, Br, I)

Ellen R. Fisher, Richard H. Schultz, and P. B. Armentrout*,†

Department of Chemistry, University of Utah, Salt Lake City, Utah 84112

(Received: February 21, 1989)

Reactions of Fe^+ with CH_3X (X = Cl, Br, I) are studied by guided ion beam techniques. State-specific reaction cross sections for production of $FeCH_3^+$ and FeX^+ are presented for the ^6D ground and the ^4F first excited states of Fe^+. The overall behavior seen in these reactions is similar to that seen in the analogous reactions of Co^+ and Ni^+, discussed in the preceding paper in this issue. The two states of Fe^+ exhibit large differences in reactivity, with the ^4F state generally being more reactive than the ^6D state for production of FeX^+ and $FeCH_3^+$. The only exception is for the exothermic formation of $FeCH_3^+$ below 0.7 eV in the CH_3I system. We postulate that this is due to a potential energy surface crossing that is avoided at low kinetic energies due to spin–orbit interactions and is permitted at higher energies. Analysis of the threshold behavior of the endothermic reactions provides two determinations of $D°(Fe^+–CH_3) = 2.49 \pm 0.13$ and 2.47 ± 0.07 eV, in good agreement with previous values. Lower limits are placed on the bond energies for Fe^+–X.

Introduction

Several studies in our laboratory have been directed at elucidating thermodynamic and mechanistic information about transition-metal hydrides and alkyls in an attempt to determine state-specific reactivity as well as periodic trends in reactivity.[1] Investigation of the reactions of Fe^+ with molecular hydrogen revealed that the ^4F first excited state of Fe^+ is more than an order of magnitude more reactive than the ^6D ground state.[2] This behavior is easily explained by using simple molecular orbital arguments that can also rationalize the behavior of *all* of the first-row transition-metal ions. For Fe^+, the significant difference between the ^6D ($4s3d^6$) and ^4F ($3d^7$) states is the occupancy of the 4s orbital. The occupied 4s orbital of the ground state leads to repulsive interactions with the filled σ_g orbital of the H_2 molecule. Thus, the ground state reacts inefficiently. The first excited state avoids this repulsion and therefore reacts efficiently via a direct process.[2]

This strong correlation between electronic state and reactivity of Fe^+ was also found to be true for the endothermic reactions of Fe^+ with small alkanes.[3] For exothermic reactions of Fe^+ with propane, however, it is the ground state that is more reactive at low kinetic energies, although at higher kinetic energies, it is once again the first excited state that is more reactive. This behavior has been attributed to a crossing between quartet and sextet surfaces which is avoided due to spin–orbit mixing at low kinetic energies but is permitted at higher energies.

In this paper, we extend these studies by using guided ion beam techniques to examine the reactions of Fe^+ with methyl chloride, methyl bromide, and methyl iodide. The kinetic energy dependent reaction cross sections are presented for both $Fe^+(^4F)$ and $Fe^+(^6D)$, and comparisons are made between the reactivity displayed by Fe^+ in these systems with that seen with H_2 and the small alkanes. In addition to the state-specific results, comparisons are also made between the reactions of Fe^+ with the methyl halides and the results of our study involving Co^+ and Ni^+.[4]

Experimental Section

The ion beam apparatus used in these experiments has been described in detail elsewhere.[5] Conditions for these experiments

---

† NSF Presidential Young Investigator, 1984–1989. Alfred P. Sloan Fellow. Camille and Henry Dreyfus Teacher-Scholar, 1987–1992.

(1) (a) Elkind, J. L.; Armentrout, P. B. *Inorg. Chem.* **1986**, *25*, 1078–1080. (b) Elkind, J. L.; Armentrout, P. B. *J. Phys. Chem.* **1987**, *91*, 2037–2045. (c) Armentrout, P. B.; Georgiadis, R. *Polyhedron* **1988**, *7*, 1573–1581.

(2) Elkind, J. L.; Armentrout, P. B. *J. Am. Chem. Soc.* **1986**, *108*, 2765–2767. Elkind, J. J.; Armentrout, P. B. *J. Phys. Chem.* **1986**, *90*, 5736–5745.

(3) Schultz, R. H.; Armentrout, P. B. *J. Phys. Chem.* **1987**, *91*, 4433–4435. Schultz, R. H.; Elkind, J. L.; Armentrout, P. B. *J. Am. Chem. Soc.* **1988**, *110*, 411–423.

(4) Fisher, E. R.; Sunderlin, L. S.; Armentrout, P. B. *J. Phys. Chem.*, preceding paper in this issue.

0022-3654/89/2093-7382$01.50/0